

This is a self-archived – parallel published version of an original article. This version may differ from the original in pagination and typographic details. When using please cite the original.

AUTHOR	Marja Malkamäki, Adrie J.J. Bos, Pieter Dorenbos, Mika Lastusaari, Lucas C.V. Rodrigues, Hendrik C. Swart, Jorma Hölsä
TITLE	Persistent luminescence excitation spectroscopy of BaAl <sub>2</sub> O <sub>4</sub> :Eu <sup>2+</sup> , Dy <sup>3+</sup>
YEAR	2020. Vol 593.
DOI	<a href="https://doi.org/10.1016/j.physb.2019.411947">https://doi.org/10.1016/j.physb.2019.411947</a>
VERSION	Author's accepted manuscript
COPYRIGHT	License: <a href="#">CC BY NC ND</a>
CITATION	Marja Malkamäki, Adrie J.J. Bos, Pieter Dorenbos, Mika Lastusaari, Lucas C.V. Rodrigues, Hendrik C. Swart, Jorma Hölsä, Persistent luminescence excitation spectroscopy of BaAl <sub>2</sub> O <sub>4</sub> :Eu <sup>2+</sup> , Dy <sup>3+</sup> , Physica B: Condensed Matter, Volume 593, 2020, 411947, ISSN 0921-4526, <a href="https://doi.org/10.1016/j.physb.2019.411947">https://doi.org/10.1016/j.physb.2019.411947</a> ( <a href="http://www.sciencedirect.com/science/article/pii/S0921452619308270">http://www.sciencedirect.com/science/article/pii/S0921452619308270</a> )

# Persistent Luminescence Excitation Spectroscopy of $\text{BaAl}_2\text{O}_4\text{:Eu}^{2+},\text{Dy}^{3+}$

**Marja Malkamäki<sup>1</sup>, Adrie J.J. Bos<sup>2</sup>, Pieter Dorenbos<sup>2</sup>, Mika Lastusaari<sup>1</sup>,**

**Lucas C.V. Rodrigues<sup>3</sup>, Hendrik C. Swart<sup>4</sup>, Jorma Hölsä<sup>1,3,4,5,\*</sup>**

<sup>1</sup> University of Turku, Department of Chemistry, and Turku University Centre for  
Materials and Surfaces, FI-20014 Turku, Finland

<sup>2</sup> Delft University of Technology, Faculty of Applied Sciences, 2628 CN Delft, the  
Netherlands

<sup>3</sup> University of São Paulo, Institute of Chemistry, BR-05508-000 São Paulo, SP,  
Brazil

<sup>4</sup> University of the Free State, Department of Physics, Bloemfontein ZA-9300, South  
Africa

<sup>5</sup> Polish Academy of Sciences, Institute of Low Temperature and Structure  
Research, PL-50-422 Wrocław, Poland

---

\* Corresponding author: Jorma Hölsä, mailing address: University of the Free State, Department of Physics, Bloemfontein ZA-9300, South Africa, tel: +27(0)612602331, fax: +27(0)514013507, e-mail: jholso@utu.fi

\* Paper presented in part at the 8<sup>th</sup> South African Conference on Photonic Materials (SACPM-2019) held at the Kariëga Game Reserve, May 6-10, 2019, Kariëga Game Reserve, South Africa.

## Abstract

$\text{BaAl}_2\text{O}_4:\text{Eu}^{2+},\text{Dy}^{3+}$  is related, both by structure and luminescence, to one of the best persistent luminescent phosphors,  $\text{SrAl}_2\text{O}_4:\text{Eu}^{2+},\text{Dy}^{3+}$ . At room temperature (RT), the green persistent emission of  $\text{BaAl}_2\text{O}_4:\text{Eu}^{2+},\text{Dy}^{3+}$  remains visible for hours after ceasing irradiation. Similar to  $\text{SrAl}_2\text{O}_4$ ,  $\text{BaAl}_2\text{O}_4$  with hexagonal  $P6_3$  structure, has two  $\text{M}^{2+}$  sites, but, limited optical activity from the 2<sup>nd</sup> site is observed in the emission of  $\text{BaAl}_2\text{O}_4:\text{Eu}^{2+},\text{Dy}^{3+}$  - even at 77 K. Using combined approach of photoluminescence, thermoluminescence (TL), and persistent (excitation) luminescence measurements, the origin and properties of persistent luminescence of  $\text{BaAl}_2\text{O}_4:\text{Eu}^{2+},\text{Dy}^{3+}$  were studied in detail. Ultraviolet (UV) excited and persistent emission are identical and no contribution from the  $\text{Eu}^{2+}$  in the high-symmetry Ba site was observed. TL excitation spectra clarified the unstructured conventional excitation spectrum; now it is evident that defects or the  $\text{Dy}^{3+}$  co-dopant do not contribute to persistent luminescence *via* direct energy absorption. Mechanisms for persistent luminescence should thus be revised.

Keywords:  $\text{BaAl}_2\text{O}_4$ ,  $\text{Eu}^{2+}+\text{Dy}^{3+}$  co-doping, persistent luminescence, thermoluminescence, excitation

## 1 Introduction

In persistent luminescence, the material continues to emit for several hours after the irradiation source has been removed [1]. This phenomenon is used in many applications such as traffic and emergency signs, watches, clocks, textile printing and, more recently, in Near Infra-Red (NIR) emitting biomedical applications. It can also be employed in sensors and thermometers. There exists a wide variety of different persistent luminescence materials such as silicates, aluminates, oxides and even sulfides. The most performant materials are the  $\text{Eu}^{2+}$  and  $\text{Dy}^{3+}$  doped aluminates that can emit in excess of 24 h [2].

Persistent luminescence is due to defects in the structure of the material. These defects can be eg lattice distortions and substitutional sites which are created into the structure with co-doping or introducing by other means structural disorder [3]. The defects act as sites where the charge carriers (electrons and holes) are trapped following irradiation. After the irradiation has been removed, charge carriers are released from the traps with the aid of thermal energy and the emitter is returned to the ground state with long delay by emitting radiation.

Thermoluminescence (TL), also called as thermally stimulated luminescence (TSL), is a method to study the trap structure of materials [4,5]. In TL, the material is first irradiated with eg UV (or  $\beta$  or X- ray) radiation for a selected length of time at low temperature, eg below RT. Then the material is heated with a constant heating rate and the emission (or detailed emission spectrum) is measured simultaneously. The former output leads to a TL glow curve in which the emission (or even entire emission spectrum) is presented as a function of temperature.

There are three pivotal factors regulating persistent luminescence output: excitation, emission and duration of emission. The latter two are trivial to measure and can be

done in most cases even with visual perception in a very short time. The excitation is a much more difficult process to detect and grasp. In conventional excitation spectroscopy, it is always uncertain if the excitation spectrum (usually in UV and/or blue ranges) is really due to excitation of persistent luminescence or only that of conventional luminescence. Moreover, if persistent luminescence is (very) strong, the conventional luminescence spectrum is flattened down due to high background and low signal-to-noise ratio. Difference in techniques to the emission is thus both fundamental and practical. Evidently, special, and probably very time consuming, technique(s) must be used to obtain reliable excitation data for persistent luminescence.

In this work, the  $\text{BaAl}_2\text{O}_4\text{:Eu}^{2+},\text{Dy}^{3+}$  persistent luminescence materials, prepared with a solid state (SS) reaction, were studied using a variety of methods.  $\text{BaAl}_2\text{O}_4\text{:Eu}^{2+},\text{Dy}^{3+}$  is the heaviest though the least efficient persistent luminescent material in the  $\text{MAl}_2\text{O}_4\text{:Eu}^{2+},\text{R}^{3+}$  (M: Ca, Sr, Ba) series. Low efficiency may be attributed to the hygroscopic host material and/or polymorphic structure [6] which both may deteriorate persistent excitation and emission through a change in the trap structure thus shortening the persistent duration as well. On the other hand, the high Ba content of these materials allows for a specific application: *X-ray induced persistent luminescence*. The use of X-rays brings additional emission power (through higher storage of energy) though there are evident disadvantages due to the use of X-ray irradiation (and Ba compounds): increased radiation damage (and increased *acute* toxicity [7] – not only because Ba is a heavy metal).

The crystal structure and purity of the  $\text{BaAl}_2\text{O}_4\text{:Eu}^{2+},\text{Dy}^{3+}$  materials was confirmed with the X-ray powder diffraction (XPD). The photo- as well as persistent luminescence properties after UV and  $\beta$  irradiation were studied. The glow curves and emission

spectra were measured after each change of the irradiating UV-vis wavelength. Using the latter results the TL excitation [8] spectra (TLES) were constructed. The 3D persistent excitation spectroscopy is expected to throw more light on the persistent properties of  $\text{BaAl}_2\text{O}_4:\text{Eu}^{2+},\text{Dy}^{3+}$  under X-ray,  $\beta$  and UV irradiation than the simple TL measurements. The most significant contribution of the present work to the ever-increasing pool of knowledge on persistent luminescence materials is to emphasize the importance of the excitation characteristics of the phosphors as well as indicate the difficulties to measure reliable excitation spectra. So far the trivial studies of the emission spectra and emission duration have overwhelmed the investigations of the equally - if not the most - important step of the persistent luminescence processes: the excitation.

## 2 Experimental

### 2.1 Materials and Methods

The  $\text{BaAl}_2\text{O}_4:\text{Eu}^{2+},\text{Dy}^{3+}$  materials were prepared with appropriate solid state reactions using the following reactants:  $\text{BaCO}_3$  (*Pro analysis*, Merck),  $\text{Al}_2\text{O}_3$ , (99.99 % - 4N, Sigma-Aldrich),  $\text{Eu}_2\text{O}_3$ , (4N, Double pilots group) and  $\text{Dy}_2\text{O}_3$  (4N, Rhodia). The  $\text{Eu}^{2+}$  and  $\text{Dy}^{3+}$  amounts were both one mole-% of the  $\text{Ba}^{2+}$  amount. Stoichiometric amounts of starting materials were ground together using a ball mill or an agate mortar. The mixtures were fired at two stages in a reducing  $\text{N}_2 + 10\% \text{H}_2$  gas sphere - 1 h @ 900 °C and 4 h @ 1300 °C.

#### 2.1.1 X-Ray Powder Diffraction

Phase purities and crystal structures of the materials were analysed using the X-ray powder diffraction (XPD) measurements. The XPD patterns were collected at RT

between 4 and 100° (in 2 $\theta$ ) with a Huber 670 image plate Guinier camera (Cu K $_{\alpha 1}$  radiation, 1.5406 Å). The data collection time was 15 min followed by ten scans of the image plate. A Ge crystal was used as a monochromator. The measured XPD patterns were compared to the calculated ones obtained using the program PowderCell [9] and appropriate crystal structure data [10].

### 2.1.2 UV Excited and Persistent Luminescence

The photoluminescence emission and excitation spectra at RT and 77 K were measured using a Varian Cary Eclipse spectrometer with a 15 W Xe lamp as the excitation source. The persistent luminescence emission spectra were measured using the same spectrometer. For the latter experiments, the material was first excited with a 4 W UVP UVGL-25 UV lamp (@ 254 nm, for 5 minutes). The persistent luminescence emission spectrum was measured with a delay of one min after shutting down the irradiation source. As an alternative to UV irradiation, the materials were also irradiated with  $\beta$  particles for 10 min using a  $^{90}\text{Sr}/^{90}\text{Y}$  source.

### 2.2 Persistent Luminescence Excitation

The TL measurements above RT were carried out with a Risø TL/OSL reader model DA-15A/B (@ Delft University of Technology, Faculty of Applied Sciences) equipped with an EMI 9635QA PM tube (sensitive in 200-650 nm) and a BG39 (or KG3) filter in front of the photomultiplier tube (PMT). A constant heating rate (5 °Cs $^{-1}$ ) was used. The TL measurements were started immediately after shutting down the irradiation source. The photon beam was produced with a 150 W Xe arc lamp (Hamamatsu L2273) and a 0.125 m monochromator (Oriel Cornerstone<sup>TM</sup> 130) giving a wavelength

resolution of 0.8 nm with 0.1 mm slit widths. The samples were pressed as pellets before measurements.

### 3 Results and Discussion

#### 3.1 Purity and Structure of Materials

The  $\text{BaAl}_2\text{O}_4\text{:Eu}^{2+},\text{Dy}^{3+}$  materials considered crystallized in the hexagonal structure (space group (SP):  $P6_3$ , #173, Z: 8) with  $a$ : 10.449 and  $c$ : 8.793 Å [11]. No impurities were observed as proven by the XPD patterns (Fig. 1). The hexagonal structure of  $\text{BaAl}_2\text{O}_4$  has two different  $\text{Ba}^{2+}$  sites [10,11]; one 6-fold site of low symmetry (with no symmetry at all) and another 2-fold site of high trigonal symmetry. It should be noted, however, that the host,  $\text{BaAl}_2\text{O}_4$ , shows pronounced tendency to polymorphic forms - more or less close to the hexagonal  $P6_3$  “parent” form.

Unfortunately, neither the conventional XPD measurements nor the calculated ICDD PDF-2 “reference” patterns (based on the corresponding ICSD data [12]) are sophisticated enough to distinguish at RT between the two main hexagonal forms with SPs  $P6_3$  (#173) and  $P6_322$  (#182). The differences are just next to nothing: slight changes in reflection intensities which may well be due to (or masked by) eg preferred orientation. Still another  $\text{BaAl}_2\text{O}_4$  phase with overall orthorhombic/(monoclinic?) structure (SP:  $P2_12_12_1$  #19) [13] has been identified with (neutron) powder diffraction (splitting of some reflections indicate lowering from the hexagonal structure). Even farther away from the hexagonal  $\text{BaAl}_2\text{O}_4$ , a cubic  $\text{BaO}\cdot\text{Al}_2\text{O}_3\cdot\text{H}_2\text{O}$  (SP:  $\text{Pm}3\text{m}$ , #221;  $a = 9.638$  Å) [14] risks to be encountered insofar the humidity attacks the anhydrous  $\text{BaAl}_2\text{O}_4$ . Eventually, a High-Temperature XPD study [6] gave at least five rather similar XPD patterns for the same  $\text{BaAl}_2\text{O}_4\text{:Eu}^{2+},\text{Dy}^{3+}$  sample in the temperature range between RT and 260 °C – and one with split reflections, indeed.



The dopant concentrations ( $\text{Eu}^{2+}$  &  $\text{Dy}^{3+}$ : 1 mol-% each) are too low to be observed either in the reflection intensities or the reflections'  $2\theta$  positions, at least partly because of the high absorption of Eu (and Dy) of the Cu  $K_{\alpha 1}$  radiation used in XPD. The scattering power of the dopants is thus too weak despite slightly higher number of electrons (Ba: 56; Eu: 63 and Dy: 66) to compensate the increased X-ray absorption. A change in the reflections'  $2\theta$  positions due to the doping used here, is also small because of the relatively high FWHM of the reflections (because of the solid state synthesis) and the small difference in the ionic sizes [15] between  $\text{Ba}^{2+}$ ,  $\text{Eu}^{2+}$  and  $\text{Dy}^{3+}$ . This ensured good solid solubility of the dopants in the  $\text{BaAl}_2\text{O}_4$  host though.

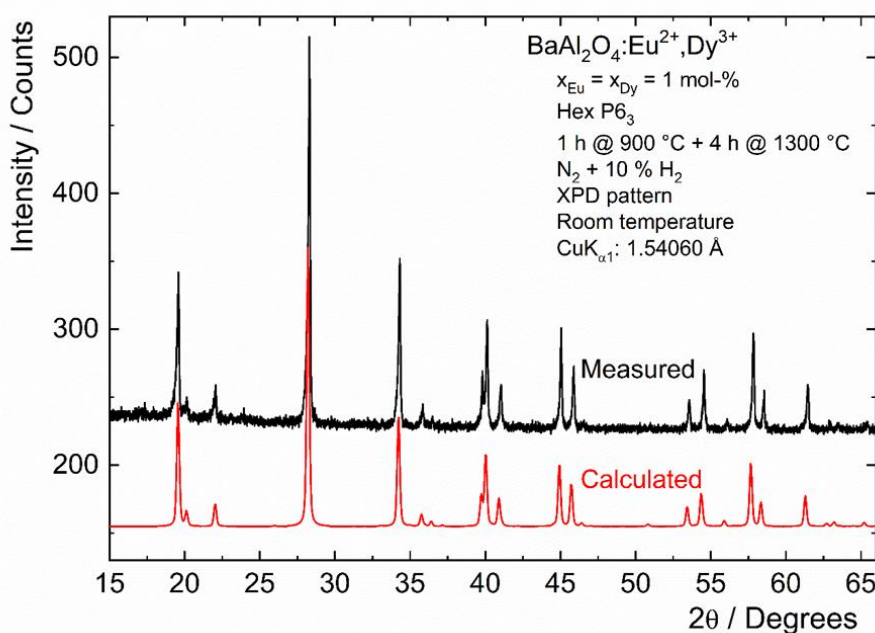


Figure 1. Measured and calculated [9,10] X-ray powder diffraction patterns of  $\text{BaAl}_2\text{O}_4:\text{Eu}^{2+},\text{Dy}^{3+}$ .

### 3.2 Photoluminescence

Since the emission spectra of  $\text{BaAl}_2\text{O}_4:\text{Eu}^{2+},\text{Dy}^{3+}$  are rather abundant in the literature, they are dealt with here only briefly. The emission spectra (Fig. 2, right) consist of a

broad emission band centered at 495 and 510 nm at RT and 77 K, respectively ( $\lambda_{\text{exc}}$ : 330 nm). Emission is due to the  $4f^65d^1(^2D) \rightarrow 4f^7(^8S_{7/2})$  transition of  $\text{Eu}^{2+}$ . No additional emission bands were observed in the spectra despite the fact that the  $\text{BaAl}_2\text{O}_4$  material has two Ba sites with different site symmetry but with the same coordination number 9 [10,11]. This observation is in contrast to an earlier study [16] where a shoulder in the lower energy side (@ 540 nm) of the main emission at 510 nm was observed at 4.2 K. The shoulder was convincingly assigned to emission from  $\text{Eu}^{2+}$  in the minority high-symmetry site. In the present study, the FWHM band width of the main emission is possibly large enough to mask entirely the band due to the minority  $\text{Eu}^{2+}$  species. The FWHM band width may be larger because of the additional structural distortions created by the  $\text{Dy}^{3+}$  co-dopant, as well.

Another reason to the absence of the emission from the high-symmetry site is offered by an enhanced energy transfer to the main emission site. Since the nominal Eu concentration is the same as in the previous study [16], the enhanced energy transfer means shortening of the  $\text{Eu}^{2+}$ - $\text{Eu}^{2+}$  distances which occur through clustering of the  $\text{Eu}^{2+}$  species. This may take place due to the inhomogeneous distribution of  $\text{Eu}^{2+}$  ions due to preparation conditions. Alternatively, the  $\text{Dy}^{3+}$  co-dopant (absent in [16]) may have an effect on this distribution, as well.  $\text{Dy}^{3+}$  in the  $\text{Ba}^{2+}$  site has an extra positive charge (but not equal to 1!) and can form clusters with other charged defects. A small  $\text{Eu}^{2+}$  in a large  $\text{Ba}^{2+}$  site induces a deficit of positive charge despite the same nominal charge and serves as a defect with negative charge. Clustering of these two species is enhanced by the long annealing times due to increase in the mobility of ions.

Eventually, although the *average* Ba-O distances are the same for the two sites [10],  $\text{Eu}^{2+}$ , being smaller than  $\text{Ba}^{2+}$ , may preferentially occupy the low-symmetry  $\text{Ba}^{2+}$  site. For this site with rather anisotropic coordination, there are several distances shorter

than the average one which may prove to be the decisive ones in the choice of  $\text{Eu}^{2+}$  occupation of smaller size.

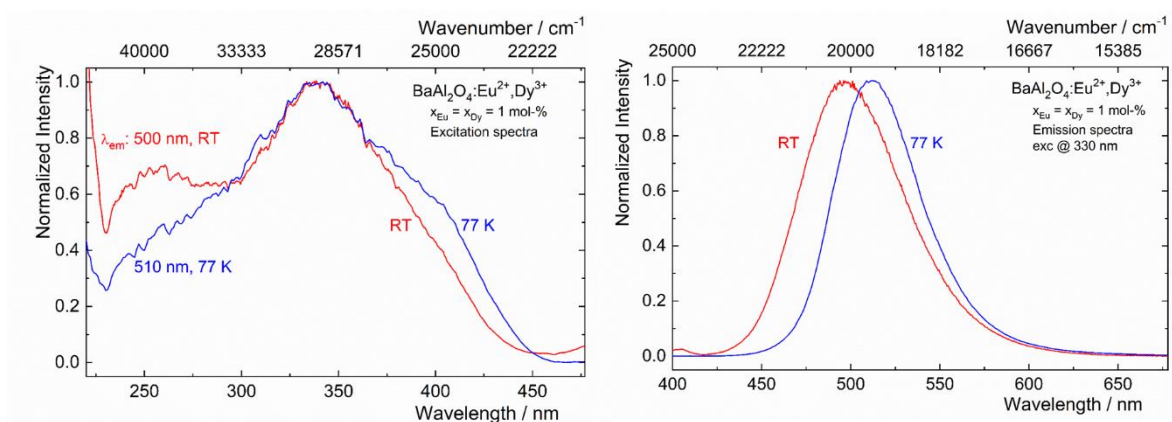


Figure 2. Excitation (left) and emission (right) spectra of  $\text{BaAl}_2\text{O}_4:\text{Eu}^{2+}, \text{Dy}^{3+}$  @ RT and 77 K.

The red-shift of the emission band with decreasing temperature (RT  $\rightarrow$  77 K) is due to the simultaneous and parallel effect of the nephelauxetic and crystal field (cf) effects. Both effects result from the shrinking of the host lattice. The latter is a consequence of strengthening of the cf effect. This increases the splitting of the  $^2\text{D}$  level and lowers the energy of the lowest  $^2\text{D}$  (emitting) level and thus the emission energy, as well. The nephelauxetic effect results from shrinking of the space available for  $\text{Eu}^{2+}$  in the  $\text{Ba}^{2+}$  site with decreasing temperature which pushes the entire  $4f^65d^1$  electron configuration to lower energy. Both effects result in lower emission energy.

The excitation spectra of  $\text{BaAl}_2\text{O}_4:\text{Eu}^{2+}, \text{Dy}^{3+}$  (Fig. 2, left) are quite similar at both temperatures though at 77 K the shoulder below 400 nm suggests slight band splitting in the spectra. The maximum excitation remains at 340 nm with emission at 500 and 510 nm at RT and 77 K, respectively. The band at ca. 260 nm is probably an artifact due to the low intensity of the Xe lamp used in the experimental setup and subsequent increased uncertainty of the intensity measurement. The prominent feature of the excitation spectra is the absence of clear band structure. In principle, the  $^2\text{D}$  level

should split up to five cf levels; for the low symmetry site  $\text{Ba}^{2+}$  exactly to five whereas for the trigonal site only to three. Combining the RT and 77 K spectra the number of bands is 4+ so the band structure may result from the low-symmetry site alone confirming the conclusions made on the emission spectra. No effect (sharp lines) due to  $\text{Dy}^{3+}$  co-dopant is observed. Due to the total  $^2\text{D}$  splitting of  $\text{ca } 20000 \text{ cm}^{-1}$ , the  $^2\text{D}$  level structure should be more visible than it is now (and the spectra presented previously [16]). Moreover, the  $^2\text{D}$  bands should show more or less clear fine structure of 7 subbands because of the  $4f^6$  part of the  $4f^65d^1$  electron configuration of  $\text{Eu}^{2+}$  - inasmuch the spectra were recorded at low temperatures, eg 4 K. At 77 K this structure may not be visible because of (or despite) the total splitting of the fine structure amounts to  $5000+ \text{ cm}^{-1}$ .

Alternatively, the severe overlap of the bands suggests excitation to the other Ba site and subsequent energy transfer to the emitting level that requires, however, short  $\text{Eu}^{2+}$ -  $\text{Eu}^{2+}$  distances contradicting with the low (1 mol-%)  $\text{Eu}^{2+}$  concentration. This was discussed already above.

The lack of clear structure in the *conventional* excitation spectra of  $\text{BaAl}_2\text{O}_4:\text{Eu}^{2+},\text{Dy}^{3+}$  is characteristic to the persistent luminescent materials with strong persistent emission. Then, during the measurement of the conventional excitation spectrum, the persistent emission contributes to a high quasi-continuous background (though weakening every minute – in principle). At the same time, due the depletion of the emitting  $\text{Eu}^{2+}$  species because of participation to the persistent luminescence process, the intensity of the  $\text{Eu}^{2+}$  bands in the conventional excitation spectrum decrease. In addition to the increase in the background emission, the signal-to-noise ratio decreases due to a decrease in emission intensity. As a result, in extreme cases, the excitation spectra may become unintelligent or, at least, very difficult to interpret.

Especially, the bands plausibly responsible for persistent luminescence, are almost impossible to identify and characterize.

In 1995 – just one year before the first preliminary report was published on the new era  $\text{MAl}_2\text{O}_4:\text{Eu}^{2+},\text{R}^{3+}$  persistent luminescence materials [17] – the effect of strong persistent luminescence on excitation spectra of seemingly innocuous phosphors was not realized. The words “persistent luminescence” (or “afterglow” or “phosphorescence” - as the persistent luminescence was called then) were mentioned not once in [16]... The persistent luminescence seems to have appeared suddenly out of the blue though the  $\text{Eu}^{2+}$  doped  $\text{MAl}_2\text{O}_4$  had been known already in the 1960s as efficient conventional phosphors but then rejected because of the strong afterglow and unfavorable thermal behavior of luminescence [18].

### 3.3 *Persistent luminescence*

The persistent emission of  $\text{BaAl}_2\text{O}_4:\text{Eu}^{2+},\text{Dy}^{3+}$  is centered at 495 nm which is almost identical with the UV excited emission band (Fig. 3, left). No trace of  $\text{Eu}^{2+}$  emission in the high-symmetry site at long wavelengths (*ie* low energy) was observed in the persistent emission, either. It is thus safe to assume that the persistent emission is due to the same  $\text{Eu}^{2+}$  center as the UV excited luminescence. It is almost a rule that no persistent emission can be observed to originate from the co-dopant, except in the rare cases when the oxidation state of the co-dopant was modified in the preparation, as for *eg*  $\text{Y}_2\text{O}_2\text{S}:\text{Eu}^{3+},\text{Ti}^{\text{IV}}$  [19,20]. The role of the co-dopant is thus usually restricted to the creation of the defects for energy storage to be subsequently used to produce persistent luminescence. The special role of a dopant with incompatible charge seems to be to form clusters between the traps (defects), emitting species and co-dopants.

This was emphasized already previously [21] and may now explain the short  $\text{Eu}^{2+}$ - $\text{Eu}^{2+}$  distances and the absence of emission of the 2<sup>nd</sup>  $\text{Eu}^{2+}$  site (see above).

Moreover, it should not be taken for granted that persistent emission could necessarily be obtained from all the *normal* (here  $\text{Eu}^{2+}$ ) emitting species present in the material. It is not excluded that the same emitting species but occupying a different site in the host structure produces persistent luminescence *at all*. The ratio of persistent luminescence may also differ from the number of the emitting centers in different sites [22]. These effects are most probably due to preferential energy transfer from the traps to the some selected emitting centers only.

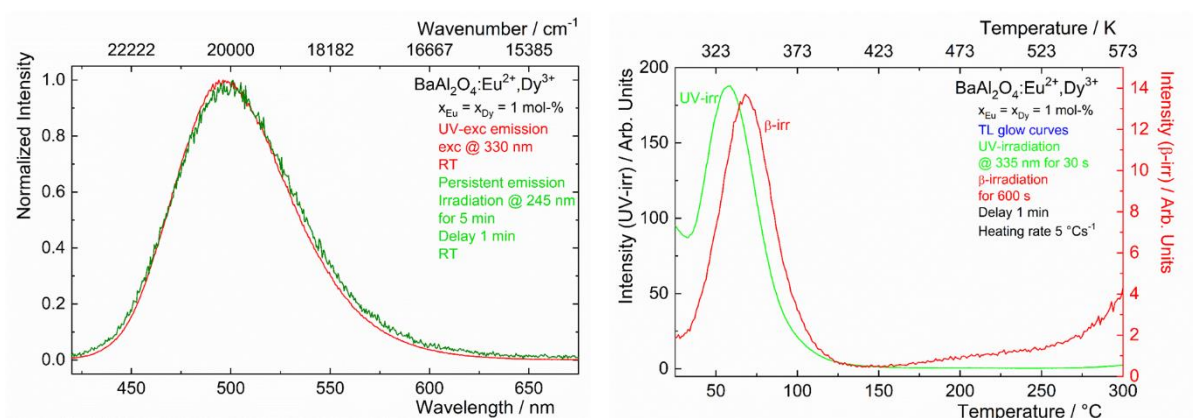


Figure 3. UV excited and persistent luminescence spectra of  $\text{BaAl}_2\text{O}_4:\text{Eu}^{2+},\text{Dy}^{3+}$  @ RT (left). TL glow curve of  $\text{BaAl}_2\text{O}_4:\text{Eu}^{2+},\text{Dy}^{3+}$  after irradiation with UV for 30 s (irradiation & excitation @ 335 nm) and with  $\beta$  radiation for 600 s.

### 3.4 Persistent Luminescence Excitation

In the TL glow curve of  $\text{BaAl}_2\text{O}_4:\text{Eu}^{2+},\text{Dy}^{3+}$  (Fig. 3, right) measured after UV irradiation (@ 335 nm), only one band at 57 °C is observed. Also after  $\beta$ -irradiation, one strong band at 68 °C exists. These TL bands are probably due to the same trap, however. The difference in the maximum temperature can be due to the different irradiation

types and times used. With  $\beta$ -irradiation, there is also a very weak band at ca. 200 °C. If this trap really exists, this deep trap cannot be filled with UV irradiation at 335 nm (ca 3.7 eV). The rise above 275 °C after  $\beta$ -irradiation is due to the increase in the background signal.

Compared to the UV irradiation, a lengthy  $\beta$ -irradiation time was needed to achieve TL data with good quality. Charging of the persistent luminescence of  $\text{BaAl}_2\text{O}_4:\text{Eu}^{2+},\text{Dy}^{3+}$  with UV irradiation is rather fast a process: the steady state can be achieved already after 30 s. Deconvolution of the TL glow curves (not shown here) yields a single trap with a depth of 0.8 eV after both UV and  $\beta$  irradiation. Results agree well with studies on the  $\text{BaAl}_2\text{O}_4:\text{Eu}^{2+},\text{Dy}^{3+}$  materials prepared with both solid state and combustion methods [23].

In the TL excitation spectra (Fig. 4) at least two bands are observed at ca. 280 and 330 nm. There is also a shoulder at ca. 380 nm. The excitation is most efficient with the 330 nm irradiation. The shape of the TL excitation spectra does not change between 50 and 100 °C (Fig. 4, left) though immediate bleaching of the traps results in weak intensity at high temperatures (above 75 °C). At temperatures higher than 100 °C, a band at ca 220 nm is detected, though this is probably an artefact due to the experimental setup. The high-energy band is close to the band gap energy of  $\text{BaAl}_2\text{O}_4$ . The complex band structure is mainly due to the splitting of the excited  $5d^1\ ^2D$  level of  $\text{Eu}^{2+}$  coupled to the structure of the  $4f^6$  levels (in fact, the electron configuration of  $\text{Eu}^{2+}$  is  $4f^65d^1$ ).

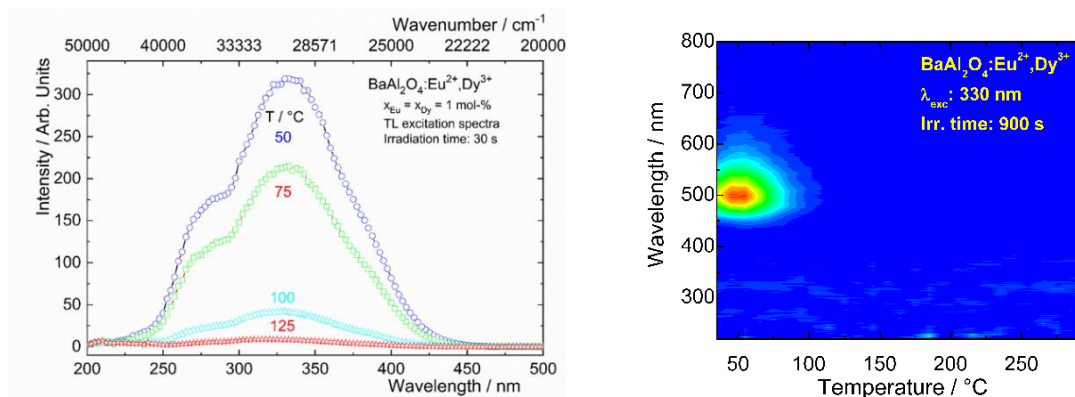


Figure 4. TL excitation spectra of  $\text{BaAl}_2\text{O}_4:\text{Eu}^{2+},\text{Dy}^{3+}$  at different temperatures (left) and contour plot of the corrected TL glow curves of  $\text{BaAl}_2\text{O}_4:\text{Eu}^{2+},\text{Dy}^{3+}$  measured after irradiation with different wavelengths (right).

Irradiation of  $\text{BaAl}_2\text{O}_4:\text{Eu}^{2+},\text{Dy}^{3+}$  with UV-vis radiation in the range from 200 to 500 nm has no effect on the shape of the TL glow curves consisting still only of a main band centred at 57 °C. The excitation spectra show little fine structure though at least two bands can be observed at 280 and 330 nm (max) with a shoulder at 380 nm. Despite the low quality of conventional excitation spectra, the persistent excitation spectra are similar to that, indicating the same origin of the bands. The huge advantage of the persistent luminescence excitation spectra, though the apparent resolution is not as good as of the conventional one, is the extreme clarity of the spectra. Now the bands can be seen without doubt and it is confirmed that the band structure is due to the  $\text{Eu}^{2+}$  centre only. Moreover, no defect or  $\text{Dy}^{3+}$  related excitation could be observed. The duty of  $\text{Dy}^{3+}$  is thus exclusively to trap the electrons and to form dopant ion clusters to enhance the transfer of charge carriers.

#### 4 Conclusions

The persistent luminescent  $\text{BaAl}_2\text{O}_4:\text{Eu}^{2+},\text{Dy}^{3+}$  phosphors with the hexagonal  $\text{P6}_3$  structure were successfully manufactured in pure form. The exact structure of the host



could not, however, be verified due to several very similar hexagonal structures. The photoluminescence and persistent luminescence are essentially identical indicating the same emitting  $\text{Eu}^{2+}$  centre; it cannot thus be excluded that only one  $\text{Eu}^{2+}$  centre (out of two) is involved in the emission. The TL excitation spectra clarified vastly the unstructured conventional excitation spectrum. No contribution from defects or the  $\text{Dy}^{3+}$  co-dopant could be observed in the TL excitation spectra.

The deconvolution of the TL glow curves yielded one trap @ 0.8 eV which is close but slightly too shallow for the use of  $\text{BaAl}_2\text{O}_4:\text{Eu}^{2+},\text{Dy}^{3+}$  as persistent luminescent phosphors at RT. The charging of the persistent luminescence of  $\text{BaAl}_2\text{O}_4:\text{Eu}^{2+},\text{Dy}^{3+}$  is a fast process which facilitates the practical use of these materials. Although the harvesting of UV radiation from 250 to 400 nm is efficient covering well the near UV part of the solar emission reaching earth's surface, the total efficiency is rather low since the portion of UV radiation in the solar spectrum is rather low, only below 20 %. Eventually, the comparison between the present PLES and those for the only  $\text{Eu}^{2+}$  doped materials published earlier, shows that the  $\text{Dy}^{3+}$  co-doping is not absolutely essential to obtain persistent luminescence. That said, the  $\text{R}^{3+}$  co-doping can boost (or abate) persistent luminescence up to several orders of magnitude [24]. This observation provides important information as far as the mechanism of co-doping is considered.

## 5 Acknowledgements

Financial support is acknowledged from the Academy of Finland (Contract No. 134459). MSc Karina Grzeszkiewicz (Polish Academy of Sciences, Institute of Low Temperature and Structure Research, PL-50-422 Wrocław, Poland) is acknowledged for providing selected ICSD (Inorganic Crystal Structure Database, FIZ Karlsruhe)

entries for BaAl<sub>2</sub>O<sub>4</sub> and related materials. PhD Taneli Laamanen (University of Turku, Department of Chemistry, FI-20014 Turku, Finland) is acknowledged for preparation of selected BaAl<sub>2</sub>O<sub>4</sub>:Eu<sup>2+</sup>,Dy<sup>3+</sup> materials.

## References

1. Li, Y., Gecevicius, M., Qiu, J.R., Long Persistent Phosphors - from Fundamentals to Applications. *Chem Soc Rev.* **45** (2016) 2090.
2. Lastusaari, M., Rodrigues, L.C.V., Swart, H.C., Hölsä, J., The Role of Defects and (Valence) Impurities in the Creation and Annihilation of (Persistent) Luminescence, 4<sup>th</sup> *Int. Workshop Persist. Photostim. Phosphors (4PPP)*, April 4 - 8, 2018, Beijing, P.R. China.
3. Hölsä, J., Lastusaari, M., Hreniak, D., Swart, H.C., Energy Trapping Sites in Persistent Phosphors, 4<sup>th</sup> *Int. Conf. Rare Earth Mater. (REMAT-2018)*, May 16-18, 2018, Wrocław Poland.
4. Bos, A.J.J., Thermoluminescence as a Research Tool to Investigate Luminescence Mechanisms, *Materials* **10** (2017) 1357.
5. Chen, R., McKeever, S.W.S., Theory of Thermoluminescence and Related Phenomena, World Scientific, Singapore, 1997, pp. 1-9, 29.
6. Hölsä, J., Swart, H.C., Rodrigues, L.C.V., Brito, H.F., Lahtinen, M., Lastusaari, M., Temperature Induced Phase Transitions in BaAl<sub>2</sub>O<sub>4</sub>. 11<sup>th</sup> *Eur. Symp. Thermal Anal. Calor. (ESTAC-11)*, Aug. 17-21, 2014, Espoo, Finland.
7. Johnson, C.H., VanTassell, V.J. Acute Barium Poisoning with Respiratory Failure and Rhabdomyolysis. *Ann. Emerg. Med.* **20** (1991) 1138.

8. Bos, A.J.J., Van Duijvenvoorde, R.M., Van der Kolk, E., Drozdowski, W., Dorenbos, P., Thermoluminescence Excitation Spectroscopy: A Versatile Technique to Study Persistent Luminescence Phosphors, *J. Lumin.* **131** (2011) 1465.
9. Kraus, W., Nolze, G. Powder Cell for Windows, Version 2.4, Federal Institute for Materials Research and Testing, Berlin, Germany, 2000.
10. Huang, S.-Y., von der Mühl, R., Ravez, J., Chaminade, J.P., Hagenmuller, P., Couzi, M., A propos de la ferroélectricité dans  $\text{BaAl}_2\text{O}_4$ , *J. Solid State Chem.* **109** (1994) 97.
11. Hörkner, W., Müller-Buschbaum, H.K., Zur Kristallstruktur von  $\text{BaAl}_2\text{O}_4$ , *Z. anorg. allg. Chem.* **461** (1979) 40.
12. The ICDD PDF-2 “reference” patterns ([www.ICDD.com](http://www.ICDD.com)) can be calculated based on the following ICSD (Inorganic Crystal Structure Database, FIZ Karlsruhe) structural information:  $\text{BaO} \cdot \text{Al}_2\text{O}_3 \cdot \text{H}_2\text{O}$  (cif file: ICSD-2550; cubic  $\text{Pm}\bar{3}\text{m}$  #221),  $\text{BaAl}_2\text{O}_4$  (ICSD-246028 orthorhombic  $\text{P2}_1\text{2}_1\text{2}_1$  #19),  $\text{BaAl}_2\text{O}_4$  (ICSD-15728 hexagonal  $\text{P6}_3\text{22}$  #182),  $\text{BaAl}_2\text{O}_4$  (ICSD-291356 hexagonal  $\text{P6}_3$  #173), and  $\text{BaAl}_2\text{O}_4$  (ICSD-291360 hexagonal  $\text{P6}_3$  #173). The ICDD PDF 2 (or PDF 4) entries for visual inspection are as follows: 82-2001 ( $\text{P6}_3$ ), 82-1350 ( $\text{P6}_3\text{22}$ ), 72-131 ( $\text{P6}_3\text{22}$ ), 72-0387 ( $\text{P6}_3\text{22}$ ), 71-1323 ( $\text{P6}_3$ ), 17-0306 ( $\text{P6}_3\text{22}$ ).
13. Larsson, A.K., Withers, R.L., Perez-Mato, J.M., Gerald, J.D.F., Saines, P.J., Kennedy, B.J., Liu, Y., On the Microstructure and Symmetry of Apparently Hexagonal  $\text{BaAl}_2\text{O}_4$ , *J. Solid State Chem.* **181** (2008) 1816.
14. Ahmed, A.H.M., Dent Glasser, L.S., King, M.G., Barium Aluminate Hydrates. VI. The Crystal Structure of ‘ $\text{BaO} \cdot \text{Al}_2\text{O}_3 \cdot \text{H}_2\text{O}$ ’. *Acta Cryst. B* **29** (1973) 1166.

15. Shannon, R.D., Revised Effective Ionic Radii and Systematic Studies of Interatomic Distances in Halides and Chalcogenides, *Acta Cryst. A* **32** (1976) 751. On-line: <http://abulafia.mt.ic.ac.uk/shannon/> (accessed on Nov 29, 2019).
16. Poort, S.M., Blokpoel, W.P., Blasse, G., Luminescence of  $\text{Eu}^{2+}$  in Barium and Strontium Aluminate and Gallate, *Chem. Mater.* **7** (1995) 1547.
17. Matsuzawa, T., Aoki, Y., Takeuchi, N., Murayama, Y., A New Long Phosphorescent Phosphor with High Brightness,  $\text{SrAl}_2\text{O}_4$   $\text{Eu}^{2+}, \text{Dy}^{3+}$ , *Electrochem. Soc.* **143** (1996) 2670.
18. Palilla, F.C., Levine, A.K., Tomkus, M.R., Fluorescent Properties of Alkaline Earth Aluminates of Type  $\text{MAl}_2\text{O}_4$  Activated by Divalent Europium, *J. Electrochem. Soc.* **115** (1968) 642.
19. Hölsä, J., Laamanen, T., Lastusaari, M., Malkamäki, M., Niittykoski, J., Zych, E., Effect of  $\text{Mg}^{2+}$  and  $\text{Ti}^{\text{IV}}$  Doping on the Luminescence of  $\text{Y}_2\text{O}_2\text{S}:\text{Eu}^{3+}$ , *Opt. Mater.* **31** (2009) 1791.
20. Luo, H., Bos, A.J.J., Dorenbos, P., Charge Carrier Trapping Processes in  $\text{RE}_2\text{O}_2\text{S}$  ( $\text{RE} = \text{La}, \text{Gd}, \text{Y}, \text{and Lu}$ ), *J. Phys. Chem. C* **121** (2017) 8760.
21. Aitasalo, T., Hölsä, J., Jungner, H., Lastusaari, M., Niittykoski, J., Thermoluminescence Study of Persistent Luminescence Materials:  $\text{Eu}^{2+}$  and  $\text{R}^{3+}$  Doped Calcium Aluminates,  $\text{CaAl}_2\text{O}_4:\text{Eu}^{2+}, \text{R}^{3+}$ , *J. Phys. Chem. B* **110** (2006) 4589.
22. Lastusaari, M., Bos, A.J.J., Dorenbos, P., Laamanen, T., Malkamäki, M., Rodrigues, L.C.V., Hölsä, J., Wavelength-Sensitive Energy Storage in  $\text{Sr}_3\text{MgSi}_2\text{O}_8:\text{Eu}^{2+}, \text{Dy}^{3+}$ , *J. Thermal Anal. Calorim.* **121** (2015) 29.
23. Rodrigues, L.C.V., Stefani, R., Brito, H.F., Felinto, M.C.F.C., Hölsä, J., Lastusaari, M., Laamanen, T., Malkamäki, M., *J. Solid State Chem.* **183** (2010) 2365.

24. Lastusaari, M., Jungner, H., Kotlov, A., Laamanen, T., Rodrigues, L.C.V., Brito, H.F., Hölsä, J., Understanding Persistent Luminescence: Rare-Earth- and  $\text{Eu}^{2+}$ -Doped  $\text{Sr}_2\text{MgSi}_2\text{O}_7$ , *Z. Naturforsch. b* **69** (2014) 171.